GEOPHYSICAL RESEARCH LETTERS, VOL. 27, NO. 15, PAGES 2197-2200, AUGUST 1, 2000

Shortwave Direct Radiative Forcing of Biomass Burning Aerosols Estimated using VIRS and CERES data

Sundar A. Christopher, Joyce Chou, Jianglong Zhang, Xiang Li, Todd. A. Berendes and Ronald M. Welch

Department of Atmospheric Sciences, University of Alabama, Huntsville, Alabama

Abstract. Using collocated data from the Visible Infrared Scanner (VIRS) and the Clouds and the Earth's Radiant Energy Budget Scanner (CERES) from the Tropical Rainfall Measuring (TRMM) satellite, observational estimates of the instantaneous Shortwave Aerosol Radiative Forcing (SWARF) of smoke aerosols at the top-of-atmosphere (TOA) are obtained for four days in May 1998 during a biomass-burning episode in Central America. The detection of smoke aerosols is demonstrated using VIRS imagery. Assuming a single scattering albedo (ω_o) of 0.86 (at 0.63 μm) that is representative of absorbing aerosols, smoke optical thickness ($\tau_{0.63}$) is retrieved over ocean areas. The average $\tau_{0.63}$ for these four days was 1.2 corresponding to a SWARF value of -68 Wm^{-2}. The SWARF changes from -24 to -99 Wm^{-2} as $\tau_{0.63}$ changes from 0.2 to 2.2. Global observational estimates of biomass burning aerosol radiative forcing can be obtained by combining data sets from TRMM and Terra satellites.

1. Introduction

During April and May 1998, large amounts of aerosols were released into the atmosphere from a biomass-burning episode in Central America. The smoke aerosols from these fire events were transported over long distances, even reaching the northern latitudes of the continental United States. These aerosols affect the radiative balance of the earth-atmosphere system by reflecting sunlight back to space, called the direct radiative effect [*Penner et al.,* 1992], and by acting as cloud condensation nuclei and modifying the shortwave reflective properties of clouds, called the indirect radiative effect [*Kaufman and Fraser,* 1997]. The difficulties in quantifying these effects and some strategies are addressed in a National Research Council Report [*NRC,* 1996].

There are several approaches for estimating the direct radiative effect of biomass burning. Some commonly used methods include the use of radiative transfer equations [*e.g., Penner et al.* 1992] and climate model simulations [*e.g. Hansen et al.,* 1998] to estimate global values of aerosol radiative forcing. In this paper, using two new data sets from the Tropical Rainfall Measuring Mission (TRMM), we demonstrate an observational approach for estimating the regional instantaneous direct radiative impact of biomass burning aerosols. The two data sets are the Visible Infrared Scanner (VIRS) and the Clouds and the Earth's Radiant Energy System (CERES) scanner. The VIRS is a five channel scanning radiometer that measures reflected and emitted radiation from the earth-atmosphere system from a 350-km orbit with a swath width of 720 km at a nadir spatial resolution of 2.11 km [*Kummerow et al.*, 1998]. The five channels are centered at 0.63 ($\rho_{0.63}$), 1.6 ($\rho_{0.63}$), 3.75 ($T_{3.75}$), 10.7 ($T_{10.7}$), and 12.0 ($T_{12.0}$), μm, where ρ and T denotes reflectivity and brightness temperature respectively. Since the 3.75 μm channel has an emitted and a reflected component, a sixth channel ($\rho_{3.75}$) is estimated by removing the thermal emission using the 10.7 μm channel [*Kaufman and Nakajima,* 1993]. The CERES scanner is a broadband instrument that measures the TOA radiance in three bands (0.3 to > 50 μm (total), 0.3 - 5 μm (shortwave), 8-12 μm (longwave)) at a spatial resolution of about 10 km at nadir [*Wielicki et al.*, 1996]. The measured broadband radiances are converted to TOA fluxes using angular dependence models [*Wielicki and Green,* 1986] that were developed as part of the Earth radiation Budget Experiment (ERBE) program.

Paper number 1999GL010923.
0094-8276/00/1999GL010923$05.00

2. Method

Biomass burning aerosols are identified using the VIRS (level 1B, version 4) data. These data are then collocated with the broadband TOA fluxes from the CERES (ERBE-like) product. While several quality control procedures are currently being implemented to improve these data, we use the presently available version of the VIRS and CERES data to examine the instantaneous shortwave aerosol radiative forcing (SWARF) of biomass burning aerosols. Four days in May 1998 (4^{th}, 6^{th}, 9^{th} and 13^{th}) over Central America, between 90-110W in longitude and 15-30N in latitude, are examined. Since the majority of the biomass burning aerosols are dominated by accumulation mode particles [*Reid et al.,* 1998], $\rho_{0.63}$ is sensitive to smoke aerosol loading in the atmosphere while $\rho_{1.6}$ and $\rho_{3.7}$ are less sensitive [*Kaufman et al.,* 1998; *Chu et al.,* 1998] to the smoke aerosols. In contrast, the reflection of solar radiation by low-level water clouds in the 1.6 μm and 3.7 μm channels are dependent upon their particle size [*Nakajima and King,* 1990]. These different spectral signatures [*Kaufman and Fraser,* 1997] are used to separate the VIRS imagery into six classes, namely, 1) smoke over water, 2) smoke over land, 3) cloud over water, 4) cloud over land, 5) smoke and cloud free land, and 6) smoke and cloud free water. Over water, clouds are identified from VIRS imagery using the following criteria: $\rho_{0.63} > 0.10$, $\rho_{1.6} > 0.08$, and $T_{10.7} < 300K$. These thresholds identify cloudy pixels with cloud top temperatures colder than 300K and with TOA visible ($\rho_{0.63}$) and near-infrared reflectivity values ($\rho_{1.6}$) greater than 0.10 and 0.08, respectively. Over land, since surface reflectivity is higher in the visible and near-infrared channels when compared to ocean areas, clouds are identified using the following thresholds: $\rho_{0.63} > 0.20$, $\rho_{1.6} > 0.25$, and $T_{10.7} < 300K$. Since the reflec-

tivity of smoke aerosols is higher in the visible channel as compared to the near-infrared channel, smoke pixels over the ocean are identified by $0.10 < \rho_{0.63} > 0.45$, $\rho_{3.7} < 0.05$, $\rho_{1.6} < 0.08$ and $T_{10.7} > 281$K. These criteria identify smoke pixels with visible reflectance values between 0.10-0.45 and low TOA near ($\rho_{1.6}$) and mid-infrared (IR) reflectance ($\rho_{3.7}$) values. To identify smoke pixels over land, the following thresholds are used: $0.15 < \rho_{0.63} > 0.45$, $\rho_{3.7} < 0.09$, $\rho_{1.6} < 0.25$, and $T_{10.7} > 281$K. Additional tests are also performed for thin cirrus clouds by examining the temperature differences between the two infrared channels [*Inoue,* 1989]. These criteria for separating clouds and smoke aerosols from VIRS imagery were selected after examining the VIRS images over the period of study. However, these criteria may require some adjustments over other background types. These thresholds assume that the reflectances for the various classes are discrete in nature. However, some of the classes could be misidentified when overlaps between the different classes exist. The accuracy of the detection scheme was verified by comparing the visible imagery with the classified images.

The next step is to quantify the CERES TOA fluxes due to smoke aerosols as a function of VIRS retrieved 0.63 μm aerosol optical depth ($\tau_{0.63}$). As a first step, using a discrete ordinate radiative transfer model (DISORT), $\tau_{0.63}$ is computed over the ocean for non-sunglint areas using a look-up-table approach [*Nakajima and King,* 1990]. In this study, aerosol optical thickness retrievals are not performed over land areas. DISORT is used to compute the radiance at the TOA for a range of aerosol optical depths ($\tau_{0.63}$), and sun-satellite viewing geometries. A Lambertian surface is assumed with a channel 1 reflectivity of 0.06 and with standard atmospheric tropical temperature and water vapor profiles [*Kneisyz et al.,* 1988]. Surface anisotropy and wind speed effects are not taken into account in the current approach. The smoke aerosols are characterized as an internal mixture of viscous organic liquids surrounding a spherical black carbon core [*Ross et al.,* 1998]. The density of the black carbon core and organic shell were assigned values of 1.8 g cm^{-3} and 1.2 g cm^{-3} respectively and the mass fraction of black carbon was assumed to be 8% [*Ross et al.*, 1998]. A lognormal size distribution composed of fine-mode particles with a volume mode radius of 0.15 and a standard deviation of 1.80 was used [*Reid et al.*, 1998]. The real and imaginary part of the refractive index of the organic shell and the black carbon core were assigned values of (1.5, 0i) and (1.6, 0.4i), respectively [*Chang and Charalampopoulos,* 1990]. This yielded a ω_0 value of 0.86 at 0.63 μm that is well supported by other studies for regional smoke and aged aerosols [e.g., *Reid et al.,* 1998]. However, for non-absorbing aerosols, the single scattering albedo has larger values. It has been shown that one of the key parameters that affect aerosol optical thickness retrievals is ω_0 [*e.g., Chu et al.*, 1998]. Our calculations show that for a retrieved $\tau_{0.63}$ value of 1, a change in ω_0 (at 0.63 μm) from 0.83 to 0.89 results in a change in optical thickness from 1.16 to 0.89. Larger (smaller) values of ω_0 produce smaller (larger) aerosol optical thickness. These differences are larger at larger optical depths and lower single scattering albedos.

3. Results

Figure 1a shows an example of a VIRS image from May 9, 1998 over Central America between 1710-1717 UTC. This is a pseudo color composite with $\rho_{0.63}$ in red, $\rho_{1.6}$ in green and $\rho_{3.7}$ in blue. Water is shown in black, vegetated areas in green, clouds in white, and smoke aerosols as orange. The large spatial extent of the smoke aerosols over the Gulf of Mexico region can be seen in Fig. 1a. Also shown in the inset of Fig. 1a are the CERES TOA shortwave (SW) fluxes. The darker cloud and smoke free ocean areas have low SW flux values between 80-120 Wm^{-2}, while larger values correspond to cloud and smoke free land (130-220 Wm^{-2}), smoke over water (90-250 Wm^{-2}), and smoke over land (200-250 Wm^{-2}). The large range of SW and LW flux values over land is a function of the diversity of surface types over the area of study.

After each VIRS image is separated into different classes, the next step is to examine the TOA flux for each class from the CERES instrument. Since a CERES footprint is about 5 times larger than that of the VIRS, a group of VIRS pixels were collocated with the CERES pixel in a procedure similar to that outlined in *Christopher et al.* [1998]. To ensure overcast smoke conditions only those CERES footprints completely filled with smoke (as detected from VIRS) were used. Fig. 1b shows the relationship between the CERES longwave (LW) and CERES SW flux for each collocated pixel (roughly 10x10 km). Also shown in Fig. 1b are the standard deviations for each class. More than thirty thousand collocated samples were used in this scatter plot. The TOA SW flux of cloud and smoke free pixels over water is 100±22 Wm^{-2}. Due to higher reflectivity values, smoke pixels over ocean have larger SW flux values as compared to cloud and smoke free ocean areas. Due to warmer temperatures, the background land areas have higher LW flux values as compared to the ocean, while smoke free areas over land have larger SW flux values as compared to cloud and smoke free land areas. The VIRS $\rho_{0.63}$ values are smaller for smoke and cloud free ocean areas (0.06±0.03) as compared to smoke and cloud-free land (0.13±0.03) and smoke aerosol over ocean (0.13±0.05) and smoke aerosol over land (0.22±0.07). The $\rho_{1.6}$ values for land are 21%, due to the increased reflection from vegetated areas as compared to cloud and smoke-free ocean pixels. For smoke pixels over ocean the $\rho_{1.6}$ (0.04±0.01) and $\rho_{3.7}$ (0.02±0.01) values are smaller than the corresponding $\rho_{0.63}$ (0.13±0.05) values. On average, the CERES SW flux values for smoke over ocean areas are about 60 Wm^{-2} larger than that of background, while over land, smoke SW fluxes are larger by 90 Wm^{-2}. This difference, due to surface and aerosol properties, is used to compute shortwave aerosol radiative forcing (SWARF = S_0 (α_{clr}-α_{aer}) where S_0 denotes incoming solar flux in Wm^{-2} and α_{clr} and α_{aer} denote clear and aerosol sky albedos) [*Christopher et al.,* 1998]. The SWARF values are then quantified as a function of smoke optical thickness. A negative SWARF value indicates a net aerosol cooling effect. That is, less solar radiation is available at the surface due to the increased reflection of the smoke aerosols.

More than 8000 collocated samples over four days were used to compute the CERES SWARF of biomass burning aerosols as a function of VIRS $\tau_{0.63}$ (Fig. 1c) over ocean areas. The results are binned as a function of $\tau_{0.63}$ and the standard deviation in SWARF and $\tau_{0.63}$ is shown for each bin. Therefore for each collocated pixel identified as smoke, the average value of SW flux over ocean is used to compute the SWARF of biomass burning aerosols. Fig. 1c shows that the SWARF increases (increasingly negative) as a function of $\tau_{0.63}$. The average VIRS retrieved smoke optical thickness for the four days over the ocean was 1.2 corresponding to SWARF of -68 Wm^{-2}. A second-order polynomial fit through the points is

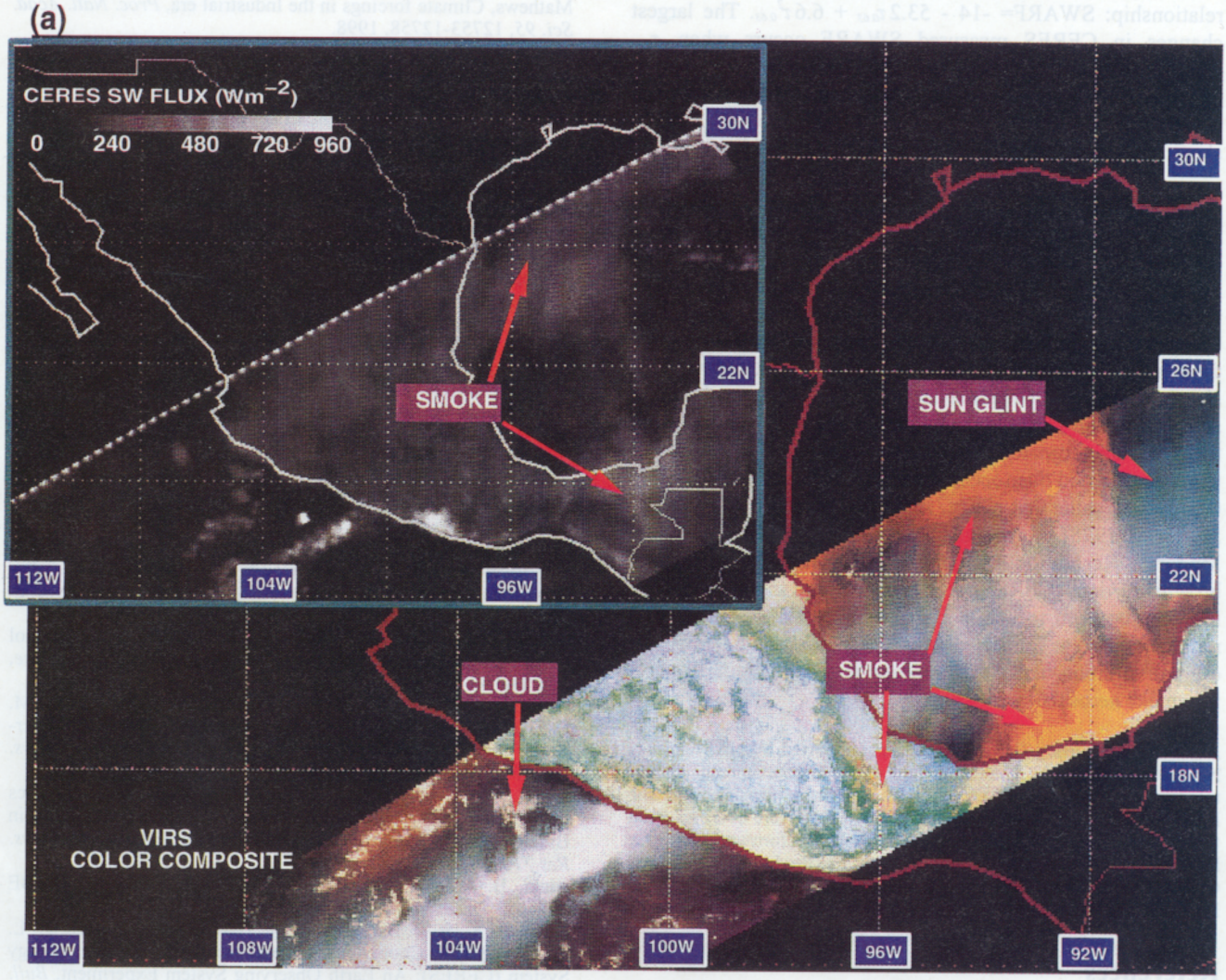

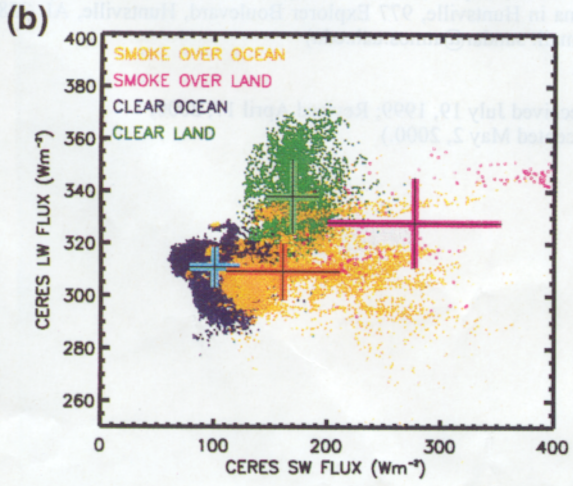

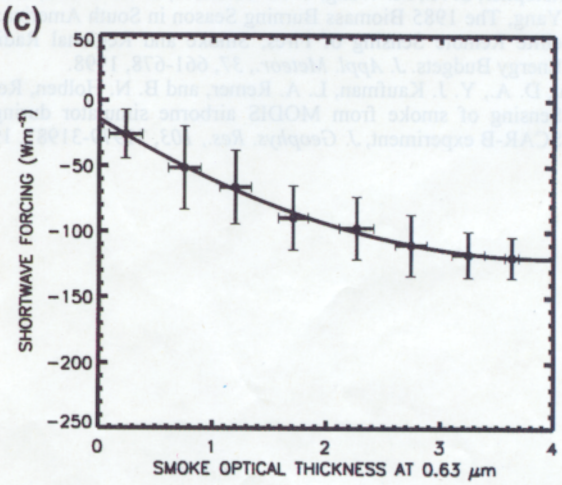

Figure 1. First results from TRMM using VIRS and CERES data, (a) VIRS pseudo color composite with channel 1 in red, channel 2 in green and the reflectance portion of channel 3 in blue. Also shown in the inset are the CERES shortwave fluxes, (b) CERES top-of-atmosphere longwave vs. shortwave fluxes for each class, (c) Shortwave aerosol radiative forcing as a function of retrieved aerosol optical depth at 0.63 μm for a single scattering albedo of 0.86.

shown by the solid line in figure 1c yielded the following relationship: SWARF= -14 - $53.2\tau_{0.63}$ + $6.6\tau^2_{0.63}$. The largest changes in CERES measured SWARF occurs when $\tau_{0.63}$ changes from 0.2 to 2.2. When VIRS retrieved $\tau_{0.63}$ changes from 0.2 to 2.2, the SWARF changes from -24 to -99 Wm^{-2}, a net change of 75 Wm^{-2}. Further changes in $\tau_{0.63}$ (2.2-3.6) show small increases in SWARF (net change of 20 Wm^{-2}).

4. Summary

Each year more than 100 Tg of aerosols are released from biomass burning, 80% of which are in tropical regions. The newly launched TRMM platform has two instruments that can be used to monitor biomass-burning aerosols and to measure their radiative impact at the TOA. Using VIRS imagery, a simple thresholding method is used to identify smoke aerosols. Using the CERES scanner data, the SWARF values at the TOA are estimated. Smoke aerosol optical thickness values are estimated over ocean areas using a ω_0 value of 0.86 (at 0.63 μm), a value that is well supported by other studies [*e.g., Reid et al.* 1998]. A synergistic use of narrowband [e.g. VIRS, Moderate Resolution Imaging Spectrometer (MODIS)] and broadband data (CERES) sets from current and future satellites can be used to obtain independent estimates of aerosol radiative forcing. Further research is needed to quantify the diurnal variation of SWARF and to improve angular models for smoke aerosols.

Acknowledgments. This research was supported by NASA grants NAGW5-7270 and NCC-8141 as part of the Global Aerosol Climatology Project. We thank Dr. Warren Wiscombe for providing the Mie code for stratified spheres. The CERES data were obtained from the NASA Earth Observing System Data and Information System, Distributed Active Archive Center (DAAC) at the Langley Research Center and the VIRS data was obtained through the Goddard Space Flight Center DAAC.

References

Chang, H., and T. T. Charalampopoulos, Determination of the wavelength dependence of refractive indices of flame soot, *Proc. R. Soc. London Ser, A., 430*, 577-591, 1990.

Christopher, S. A., M. Wang, T. A. Berendes, R. M. Welch, and S.K. Yang, The 1985 Biomass Burning Season in South America: Satellite Remote Sensing of Fires, Smoke and Regional Radiative Energy Budgets. *J. Appl. Meteor., 37*, 661-678, 1998.

Chu, D. A., Y. J. Kaufman, L. A. Remer, and B. N. Holben, Remote Sensing of smoke from MODIS airborne simulator during the SCAR-B experiment, *J. Geophys. Res., 103*, 31979-31987, 1998.

Hansen, J. E., M. Sato, A. Lacis, R. Ruedy, I. Tegen, and E. Mathews, Climate forcings in the Industrial era, *Proc. Natl. Acad. Sci. 95*, 12753-12758, 1998.

Inoue, T., Features of clouds over the tropical Pacific during Northern Hemisphere winter derived from split window measurements, *J. Meteor. Soc., Japan, 67*, 621-637, 1989.

Kaufman, Y. J., and T. Nakajima, Effect of Amazon smoke on cloud microphysics and albedo, *J. Appl. Meteor, 32*, 729-744, 1993.

Kaufman, Y. J., and R. S. Fraser, The Effect of Smoke Particles on Clouds and Climate Forcing. *Science, 277*, 1636-1639, 1997.

Kaufman, Y. J., P. V. Hobbs, V. W. J. H. Kirchoff, P. Artaxo, L. A. Remer, B. N. Holben, M. D. King, E. M. Prins, D. E. Ward, K. M. Longo, L. F. Mattos, C. A. Nobre, J. D. Spinhirne, Q. Ji, A. M. Thompson, J. F. Gleason, S.A. Christopher and S. C. Tsay, The Smoke, Clouds, and Radiation Experiment in Brazil (SCAR-B), *J. Geophys. Res., 103*, 31783-31808, 1998.

Kneizys, F. X., E. P. Shettles, L. W. Abreu, J.H. Chetwynd, G. P., Anderson, W. O. Anderson, J. E. A. Selby, and S.A. Clough, Users Guide to LOWTRAN 7, AFGL-TR-0177, 1988.

Kummerow, C., W. Barnes, T. Kozu, J. Shiue, and J. Simpson, The Tropical Rainfall Measuring Mission (TRMM) Sensor Package, *J. Atmos. Oceanic Tech., 15*, 809-817, 1998.

National Research Council (NRC), Aerosol Radiative Forcing and Climate Change, National Academy Press, Washington, DC, 200555, 161pp, 1996.

Nakajima, T., and M.D. King, Determination of the optical thickness and effective particle radius of clouds from reflected solar radiation measurements, Part 1: Theory, *J. Atmos. Sci., 47*, 1878-1893, 1990.

Penner, J.E., R. E. Dickinson, and C.A. O'Neill, Effects of aerosol from biomass burning on the global radiation budget. *Science, 256*, 1432-1434, 1992.

Reid, J. S., P. V. Hobbs, R. J. Ferek, D. R. Blake, J. V. Martins, M. R. Dunlap and C. Liousse, Physical, chemical and optical properties of regional hazes dominated by smoke in Brazil, *J. Geophys. Res., 103*, 32059-32080, 1998.

Ross, J. L., P. V. Hobbs, and B. N. Holben, Radiative characteristics of regional hazes dominated by smoke from biomass burning in Brazil: Closure tests and direct radiative forcing, *J. Geophys. Res., 103*, 31925-31942, 1998.

Wielicki, B. A., and R.N. Green, Cloud identification for ERBE radiative flux retrieval, *J. Appl. Meteor., 28*, 1133-1146, 1989.

Wielicki, B. A., B. R. Barkstrom, E. F. Harrison, R.B. Lee III, G. L. Smith and J. E. Cooper, Clouds and the Earth's Radiant Energy System (CERES): An Earth Observing System Experiment, *Bull. Amer. Meteor. Soc., 77*, 853-868, 1996.

S. A. Christopher, J. Chou, J. Zhang, X. Li, T. A. Berendes and R. M. Welch, Department of Atmospheric Sciences, University of Alabama in Huntsville, 977 Explorer Boulevard, Huntsville, AL 35807. (e-mail: sundar@atmos.uah.edu)

(Received July 19, 1999; Revised April 17, 2000;
Accepted May 2, 2000.)